View metadata, citation and similar papers at core.ac.uk
brought to you by CORE
provided by Xiamen University Institutional Repository

PHYSICAL REVIEW C **81**, 025806 (2010)

Protoneutron stars in the Brueckner-Hartree-Fock approach and finite-temperature kaon condensation

A. Li (李昂),[1] X. R. Zhou (周先荣),[1] G. F. Burgio,[2] and H.-J. Schulze[2,*]

[1]*Institute of Theoretical Physics and Astrophysics, Department of Physics, Xiamen University, Xiamen 361005, People's Republic of China*

[2]*Istituto Nazionale di Fisica Nucleare (INFN), Sezione di Catania, Via Santa Sofia 64, I-95123 Catania, Italy*

(Received 10 September 2009; published 18 February 2010)

We study the properties of hot neutrino-trapped β-stable stellar matter using an equation of state of nuclear matter within the Brueckner-Hartree-Fock approach including three-body forces, combined with a standard chiral model for kaon condensation at finite temperature. The properties of (proto)neutron stars are then investigated within this framework.

DOI: 10.1103/PhysRevC.81.025806 PACS number(s): 26.60.Kp, 26.50.+x, 13.75.Jz, 21.65.Jk

I. INTRODUCTION

One of the challenging problems in nuclear physics is to elucidate the behavior of nuclear matter in high-density and/or high-temperature environments, particularly relevant for compact stellar objects like (proto)neutron stars [(P)NSs]. Despite the importance of the structure and properties of β-stable matter at extreme densities several times normal nuclear matter density ($\rho_0 \approx 0.17$ fm^{-3}), its internal constitution and the equation of state (EOS) are not yet known with certainty.

At such densities strangeness may occur in the form of hadrons (such as hyperons or a K^- meson condensate) or in the form of strange quarks. The existence of these strange matter phases may have important consequences for the structure of compact stars and for the cooling dynamics of the PNS after a supernova explosion. With respect to kaons, the suggestion of Kaplan and Nelson [1] that, at densities high enough, the ground state of baryonic matter might contain a Bose-Einstein (BE) condensate of negatively charged kaons has prompted extensive investigations and discussions [2–17] of its implications for astrophysical phenomena in (P)NSs. In particular, the proton abundance is increased dramatically when a kaon condensate is present in NS matter, and antileptons are allowed to exist.

Some authors have treated kaon condensation within an improved chiral perturbation theory beyond tree-order calculations, and their results indicate that the critical density ρ_c^K for kaon condensation lies in the range of $2\rho_0 \lesssim \rho_c^K \lesssim 4\rho_0$. The critical density depends sensitively on the value of the strangeness content of the proton, which is still quite controversial [5,8,15,18–22].

Estimates of the relevant formation time scales [3,10] indicate that the buildup of the kaon condensate is very fast compared to the typical cooling and neutrino-diffusion time scale of several seconds characteristic for a PNS and could even play a role during the preceding supernova core collapse. Therefore, a kaon condensate might be present immediately after the formation of a PNS and influence its evolutionary history. In fact, lepton trapping in a PNS shifts the onset of kaon condensation to higher densities compared to neutrino-free matter. Also, the presence of other strange particles (e.g., hyperons) was found to push the onset of kaon condensation to higher densities, even out of the physically relevant density regime, $\rho \lesssim 1$ fm^{-3} [8,23]. This leads to the widely discussed possibility of a delayed collapse of the PNS to a black hole, when, during cooling and deleptonization evolution, the increasing softening effect of the kaons on the EOS becomes too large to stabilize an initially very massive star [4,8,9,11,24].

Obviously, for a reliable modeling of this effect the conditions of both finite temperature and lepton trapping have to be taken into account. However, most previous investigations have been done for cold matter, thus neglecting the dependence of the kaon condensation on temperature, which plays a role in significantly affecting the properties of PNSs [25–28]. Therefore we extend our previous work [16,17] to hot matter. The main goal of this article is to investigate the impact of a kaon condensate on PNS matter at finite temperature and on the final PNS observables, combining a microscopic Brueckner-Hartree-Fock (BHF) approach for the baryonic part of the matter with a standard chiral model for the kaon-nucleon contribution.

The paper is organized as follows. In Sec. II A we discuss the finite-temperature BHF approach; in Sec. II B, the standard chiral model at finite temperature. The composition of stellar matter and the EOS are presented in Sec. III, along with the equations of stellar structure. The numerical results are then reported in Sec. IV, and conclusions are drawn in Sec. V.

II. THEORETICAL MODELS

In the kaon-condensed phase of (P)NS matter, the free energy density consists of three contributions,

$$f = f_{NN} + f_{KN} + f_L, \tag{1}$$

where f_{NN} is the baryonic part, f_{KN} is the kaonic part including the contribution from the kaon-nucleon interaction, and f_L denotes the contribution of leptons e, μ, ν_e, and ν_μ and their antiparticles.

*schulze@ct.infn.it

 ©2010 The American Physical Society

A. Brueckner-Bethe-Goldstone theory at finite temperature

In the present work, we employ the BHF approach for asymmetric nuclear matter at finite temperature [27,29–32] to calculate the baryonic contribution to the EOS of stellar matter. The essential ingredient of this approach is the interaction matrix G, which satisfies the self-consistent equations,

$$G(\rho, x; E) = V + V \sum_{1,2} \frac{|12\rangle(1-n_1)(1-n_2)\langle 12|}{E - e_1 - e_2 + i0} G(\rho, x; E) \tag{2}$$

and

$$U_1(\rho, x) = \mathrm{Re} \sum_2 n_2 \langle 12|G(\rho, x; e_1 + e_2)|12\rangle_a, \tag{3}$$

where $x = \rho_p/\rho$ is the proton fraction, and ρ_p and ρ are the proton and the total baryon density, respectively. E is the starting energy and $e(k) \equiv k^2/2m + U(k)$ is the single-particle (s.p.) energy. The multi-indices 1,2 denote, in general, momentum, isospin, and spin.

The realistic nucleon-nucleon (NN) interaction V adopted in the present calculation is the Argonne V_{18} two-body force [33] supplemented by either a microscopic three-body force (TBF) based on the meson-exchange approach [34–36] (denoted micro-TBF in the following) or the phenomenological Urbana UIX force discussed in Refs. [37] and [38] (pheno-TBF), which are reduced to an effective two-body force and added to the bare potential in the BHF calculation (see Refs. [34–36] for details).

At finite temperature, $n(k)$ in Eqs. (2) and (3) is a Fermi distribution. For a given density and temperature, these equations have to be solved self-consistently along with the following equations for the auxiliary chemical potentials $\tilde{\mu}_{n,p}$,

$$\rho_i = 2 \sum_k n_i(k) = 2 \sum_k \left[\exp\left(\frac{e_i(k) - \tilde{\mu}_i}{T} \right) + 1 \right]^{-1}. \tag{4}$$

To save computational time and simplify the numerical procedure, in the following we employ the so-called *frozen correlations approximation* [27,32], that is, the correlations at $T \neq 0$ are assumed to be essentially the same as at $T = 0$. This means that the s.p. potential $U_i(k)$ for component i at finite temperature is approximated by the one calculated at $T = 0$. Within this approximation, the nucleonic free energy density has the following simplified expression:

$$f_{NN} = \sum_{i=n,p} \left[2 \sum_k n_i(k) \left(\frac{k^2}{2m_i} + \frac{1}{2} U_i(k) \right) - T s_i \right], \tag{5}$$

where

$$s_i = -2 \sum_k \left(n_i(k) \ln n_i(k) + [1 - n_i(k)] \ln[1 - n_i(k)] \right) \tag{6}$$

is the entropy density for the component i treated as a free Fermi gas with spectrum $e_i(k)$. It turns out that the assumed independence is valid to a good accuracy [27,32], at least for temperatures that are not too high, $T \lesssim 30$ MeV.

For illustration, Fig. 1 displays the EOS obtained following the procedure just discussed, for symmetric nuclear matter and purely neutron matter, adopting the micro-TBF. In the upper panels the internal energy per particle is displayed, whereas the lower panels show the free energy as a function of the baryon density, for several values of temperature between 0 and 50 MeV. We note that the free energy of symmetric matter is a monotonically decreasing function of temperature. At $T = 0$ the free energy coincides with the internal energy and the corresponding curve is just the usual nuclear matter saturation curve. On the contrary, the internal energy is an increasing function of temperature. The effect is less pronounced for pure neutron matter, owing to the larger Fermi energy of the neutrons at given density. We note that the results of this micro-TBF are always stiffer than those of the phenomenological Urbana TBF [37] used in Ref. [38].

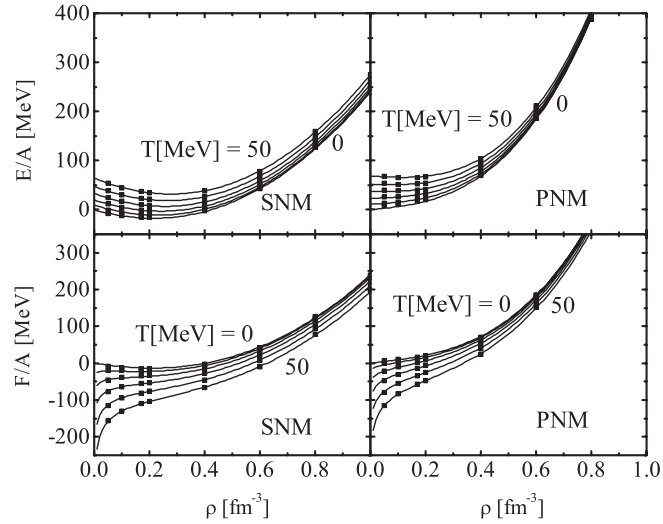

FIG. 1. Finite-temperature EOS for symmetric (left panels) and purely neutron (right panels) matter. The internal energy (upper panels) and the free energy (lower panels) are displayed as a function of the nucleon density, for temperatures ranging from 0 to 50 MeV, in steps of 10 MeV. Numerical data (symbols) and results of the fits, Eqs. (10) and (11) (curves), are shown.

For practical use, we provide analytical fits of the internal energy $E/A(T, \rho, x)$ as well as the free energy $F/A(T, \rho, x)$. It turns out that for both quantities the dependence on the proton fraction can be very well approximated by a quadratic dependence, as at zero temperature [30,39],

$$\frac{E}{A}(T, \rho, x) \approx \frac{E}{A}(T, \rho, x = 0.5) + (1 - 2x)^2 E_{\mathrm{sym}}(T, \rho), \tag{7}$$

where the symmetry energy E_{sym} can be expressed in terms of the difference in the energy per particle between pure neutron ($x = 0$) and symmetric ($x = 0.5$) matter:

$$E_{\mathrm{sym}}(T, \rho) = -\frac{1}{4} \frac{\partial (E/A)}{\partial x}(T, \rho, 0) \tag{8}$$

$$\approx \frac{E}{A}(T, \rho, 0) - \frac{E}{A}(T, \rho, 0.5). \tag{9}$$

Therefore, it is only necessary to provide parametrizations of both quantities for symmetric nuclear matter and pure neutron matter. We find that the following functional forms provide excellent parametrizations of the numerical results in

TABLE I. Parameters of EOS fits, Eqs. (10) and (11), for symmetric nuclear matter (SNM) and pure neutron matter (PNM), with both nuclear TBFs used.

	a_1	a_2	b_0	b_1	b_2	c_0	c_1	d
Micro-TBF								
E/A, SNM	81	95	−155	−139		395	81	2.09
E/A, PNM	101	73	54	−181		659	84	2.88
F/A, SNM	41	120	−115		−182	355		2.24
F/A, PNM	18	123	83		−103	631		3.02
Pheno-TBF								
E/A, SNM	105	74	−473	−464		586	381	1.26
E/A, PNM	109	64	34	−240		249	164	1.97
F/A, SNM	41	116	−180		−174	293		1.57
F/A, PNM	21	116	101		−131	191		2.62

the required ranges of density ($0.03\ \text{fm}^{-3} \lesssim \rho \lesssim 1\ \text{fm}^{-3}$) and temperature ($0\ \text{MeV} \leqslant T \leqslant 50\ \text{MeV}$):

$$\frac{E}{A}(\rho, T) = (a_1 t + a_2 t^2) + (b_0 + b_1 t)\rho + (c_0 + c_1 t)\rho^d, \tag{10}$$

$$\frac{F}{A}(\rho, T) = (a_1 t + a_2 t^2)\ln(\rho) + (b_0 + b_2 t^2)\rho + c_0 \rho^d, \tag{11}$$

where $t = T/(100\ \text{MeV})$ and E, F, and ρ are given in MeV and fm^{-3}, respectively. The parameters of the different fits are reported in Table I for both TBFs that we use.

B. Kaon condensate at finite temperature

Kaon condensation in nuclear matter has been studied intensively in a large variety of models. For the required extension to finite temperature we employ the formalism of Refs. [9] and [10], which treats fluctuations around the condensate within the framework of chiral symmetry. For low condensate amplitudes this approach is exactly equivalent to the meson-exchange mean-field models of Ref. [11], and we briefly review it now.

In the following equations, m_K and μ_K are the kaon mass and chemical potential, $f_\pi = 93$ MeV is the pion decay constant, θ is the amplitude of the condensate,

$$E_p^{\pm} = \sqrt{p^2 + \tilde{m}_K^2} \pm \tilde{\mu}_K \tag{12}$$

are the kaonic excitation energies [5,9,11,15], with

$$\tilde{m}_K = \sqrt{m_K^{*\,2}\cos\theta + b^2}, \tag{13}$$

$$\tilde{\mu}_K = \mu_K \cos\theta + b, \tag{14}$$

and

$$m_K^{*\,2} = m_K^2 + (a_1 x + a_2 + 2a_3) m_s \rho / f_\pi^2, \tag{15}$$

$$b = (1 + x)\rho/4 f_\pi^2, \tag{16}$$

are the scalar effective kaon mass and the V-spin density, respectively.

We adopt the "standard" KN interaction parameters [2,5,8,9,15], $a_1 m_s = -67$ MeV, $a_2 m_s = 134$ MeV, and $a_3 m_s = -134$, -222, and -310 MeV to perform our numerical calculations, where the different choices of a_3 correspond to different values of the strangeness content of the proton, $y = 2\langle p|\bar{s}s|p\rangle/\langle p|\bar{u}u + \bar{d}d|p\rangle \approx 0$, 0.36 [19], and 0.5 [20], in the chiral model.

We remark that the most recent lattice determination of the strangeness content of the proton [22] (as well as recent theoretical results [21]) indicates a very low value of $y < 0.05$, in strong disagreement with previous calculations [18–20]. If confirmed, such a low value would also imply a very small absolute value of a_3. Using [5] $\langle p|\bar{d}d|p\rangle \approx \langle p|\bar{u}u|p\rangle = -(a_1 + 2a_3)$ and $\langle p|\bar{s}s|p\rangle = -2(a_2 + a_3)$, we obtain

$$a_3 \approx \frac{(a_1 y/2) - a_2}{1 - y} \gtrsim \frac{-143\ \text{MeV}}{m_s}, \tag{17}$$

and kaon condensation would be strongly disfavored in the present model, as illustrated later.

The thermodynamic potential densities owing to the condensed kaons and thermal kaons are introduced as follows:

$$\omega_{KN}^c = f_\pi^2 \left[\left(m_K^{*\,2} - 2b\mu_K\right)(1 - \cos\theta) - \mu_K^2 \frac{\sin^2\theta}{2} \right], \tag{18}$$

$$\omega_{KN}^{\text{th}} = T \int \frac{d^3p}{(2\pi)^3} \ln[(1 - e^{-\beta E_p^+})(1 - e^{-\beta E_p^-})]. \tag{19}$$

Then the kaonic (charge) density q_K is given by

$$q_K = -\frac{\partial \omega_{KN}}{\partial \mu_K} \tag{20}$$

$$= f_\pi^2 [2b(1 - \cos\theta) + \mu_K \sin^2\theta] + \cos\theta \int \frac{d^3p}{(2\pi)^3} [f_B(E_p^-) - f_B(E_p^+)], \tag{21}$$

where the last term is the contribution owing to thermally excited kaons, q_K^{th}, with the Bose distribution function $f_B(E) = 1/(e^{\beta E} - 1)$.

The kaon-nucleon free energy density appearing in Eq. (1) obtained in this way is

$$f_{KN} = \omega_{KN} + \mu_K q_K \tag{22}$$

$$= f_\pi^2 \left[m_K^{*\,2}(1 - \cos\theta) + \mu_K^2 \frac{\sin^2\theta}{2} \right] + \mu_K q_K^{\text{th}} + \omega_{KN}^{\text{th}}, \tag{23}$$

and the internal energy density is

$$\epsilon_{KN} = f_{KN} + T s_K, \tag{24}$$

where the kaonic entropy density is attributable solely to the thermal kaons:

$$s_K = -\frac{\partial \omega_{KN}}{\partial T} = \beta \left(\epsilon_{KN}^{\text{th}} - \omega_{KN}^{\text{th}} \right), \tag{25}$$

with

$$\epsilon_{KN}^{\text{th}} = \int \frac{d^3p}{(2\pi)^3} [E_p^- f_B(E_p^-) + E_p^+ f_B(E_p^+)]. \tag{26}$$

One can determine the ground state by minimizing the total grand-canonical potential density ω_{KN} with respect to the condensate amplitude θ, keeping (μ_K, ρ, x) fixed. This minimization, together with the chemical equilibrium and

charge neutrality conditions, leads to the following three coupled equations [5,9,15]:

$$0 = f_\pi^2 \sin\theta\left[{m_K^*}^2 - 2b\mu_K - \mu_K^2\cos\theta\right] + \frac{\partial\omega_{KN}^{\rm th}}{\partial\theta}, \quad (27)$$

$$\mu_K = \mu_n - \mu_p = 4(1-2x)\frac{F_{\rm sym}}{A} - [a_1 m_s - (\mu_K/2)](1-\cos\theta) - \frac{1}{\rho}\frac{\partial\omega_{KN}^{\rm th}}{\partial x}, \quad (28)$$

$$q_K + q_e + q_\mu = q_p = x\rho. \quad (29)$$

Note that neglecting the thermal contribution in Eq. (27) implies $\widetilde{\mu} = \widetilde{m}$ and therefore $E_0^- = 0$ in Eqs. (12)–(14), consistent with a singularity of the BE distribution function and the existence of the condensate. We therefore also neglect the thermal contribution in Eq. (28), as is done in Ref. [9].

The lepton number density is given by ($l = e, \mu, \nu$)

$$q_l = g_l \int \frac{d^3p}{(2\pi)^3}[f_F(e_l(\boldsymbol{p}) - \mu_l) - f_F(e_l(\boldsymbol{p}) + \mu_l)], \quad (30)$$

with the Fermi distribution function $f_F(E) = 1/(e^{\beta E}+1)$, $e_l(\boldsymbol{p}) = \sqrt{m_l^2 + p^2}$, and the degeneracies $g_e = g_\mu = 2$ and $g_\nu = 1$.

The composition and the EOS of the kaon-condensed phase in chemically equilibrated (P)NS matter can be obtained by solving the coupled equations, Eqs. (27)–(29). The critical density for kaon condensation is determined as the point above which a real solution with $\theta > 0$ for the coupled equations can be found.

III. COMPOSITION AND EOS OF HOT STELLAR MATTER

In neutrino-trapped β-stable nuclear matter the chemical potential of any particle $i = n, p, K, l$ is uniquely determined by the conserved quantities baryon number B_i, electric charge Q_i, and weak charges (lepton numbers) $L_i^{(e)}$ and $L_i^{(\mu)}$:

$$\mu_i = B_i\mu_n - Q_i\mu_K + L_i^{(e)}\mu_{\nu_e} + L_i^{(\mu)}\mu_{\nu_\mu}. \quad (31)$$

For stellar matter containing nucleons, kaons, and leptons as relevant degrees of freedom, the chemical equilibrium conditions read explicitly

$$\mu_K = \mu_n - \mu_p = \mu_e - \mu_{\nu_e} = \mu_\mu + \mu_{\bar\nu_\mu}. \quad (32)$$

At a given baryon density ρ, these equations have to be solved together with the charge neutrality condition,

$$\sum_i Q_i x_i = 0, \quad (33)$$

and those expressing conservation of lepton numbers,

$$Y_l = x_l - x_{\bar l} + x_{\nu_l} - x_{\bar\nu_l}, \quad l = e, \mu\ . \quad (34)$$

Gravitational collapse calculations of the electron-degenerate core of massive stars indicate that, at the onset of trapping, the electron lepton number is $Y_e = x_e + x_{\nu_e} \approx 0.4$, with the precise value depending on the efficiency of electron capture reactions during the initial collapse stage. Also, because no muons are present when neutrinos become trapped, the constraint $Y_\mu = x_\mu - x_{\bar\nu_\mu} = 0$ is imposed. We fix the Y_l at these values in our calculations for neutrino-trapped matter. When the neutrinos have left the system, their partial densities and chemical potentials vanish and the aforementioned equations simplify accordingly.

The various chemical potentials are obtained from the total free energy density f, Eq. (1),

$$\mu_i(\{\rho_j\}) = \left.\frac{\partial f}{\partial\rho_i}\right|_{\rho_{j\neq i}}. \quad (35)$$

Once the hadronic and leptonic chemical potentials are known, one can proceed to calculate the composition of the β-stable stellar matter, and then the total pressure p, through the usual thermodynamical relation,

$$p = \rho^2\frac{\partial(f/\rho)}{\partial\rho} = \sum_i \mu_i\rho_i - f. \quad (36)$$

The stable configurations of a (P)NS can be obtained from the well-known hydrostatic equilibrium equations of Tolman, Oppenheimer, and Volkov [40] for pressure $p(r)$ and enclosed mass $m(r)$,

$$\frac{dp}{dr} = -\frac{Gm\epsilon}{r^2}\frac{[1+(p/\epsilon)][1+(4\pi r^3 p/m)]}{1-(2Gm/r)}, \quad (37)$$

$$\frac{dm}{dr} = 4\pi r^2\epsilon, \quad (38)$$

once the EOS $p(\epsilon)$ is specified, with $\epsilon = \epsilon_{NN} + \epsilon_{KN} + \epsilon_L$ the total internal energy density (G is the gravitational constant). For a chosen central value of the energy density, the numerical integration of Eqs. (37) and (38) provides the mass-radius relation.

Dynamical simulations of supernova explosions [11,41,42] show that the PNS has neither an isentropic nor an isothermal profile. For simplicity we assume a constant temperature inside the star and attach for the outer part a cold crust given in Ref. [43] for the medium-density regime ($0.001\ {\rm fm}^{-3} < \rho < 0.08\ {\rm fm}^{-3}$) and in Refs. [44] and [45] for the outer crust ($\rho < 0.001\ {\rm fm}^{-3}$). This schematizes the temperature profile of the PNS. The other extreme choice of isentropic profiles has recently been investigated within our approach [28] and no significant qualitative differences were found.

More realistic temperature profiles can be obtained by modeling the neutrinosphere both in the interior and in the external outer envelope, which is expected to be much cooler. Proper treatment of the transition from the hot interior to the cold outer part can have a dramatic influence on the mass-central density relation in the region of low central density and low stellar masses. In particular, the "minimal mass" region, typical of cold NSs [40], can be shifted in PNSs to much higher values of central density and masses. A detailed analysis of this point is given in Ref. [46], where a model of the transition region between the interior and the external envelope is developed. However, the maximum mass region that we are interested in is hardly affected by the structure of this low-density transition region [27].

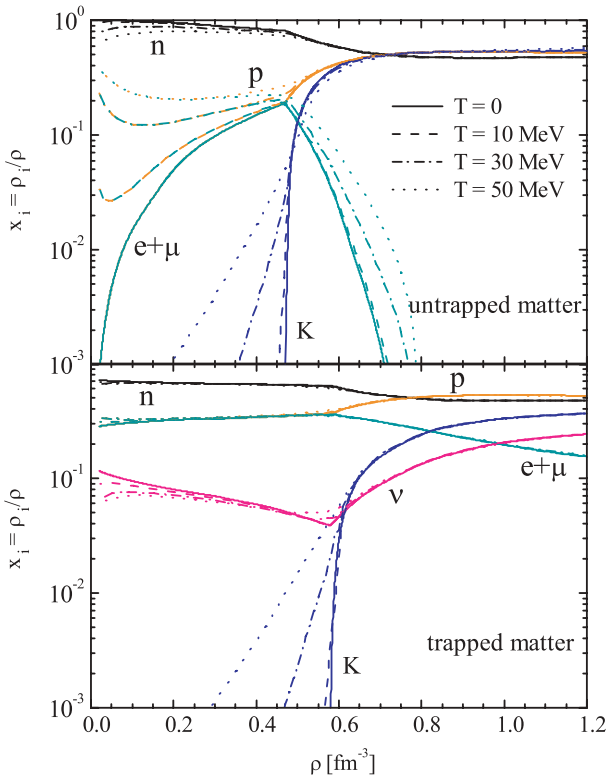

FIG. 2. (Color online) Particle fractions as a function of the baryon density in trapped ($Y_e = 0.4$; lower panel) and untrapped ($x_\nu = 0$; upper panel) β-stable matter at temperatures $T = 0$, 10, 30, and 50 MeV for $a_3 m_s = -222$ MeV and the micro-TBF.

IV. RESULTS

In the following we present the results of our numerical calculations regarding the composition of PNS matter and the structure of PNSs.

A. Composition of stellar matter

Figure 2 displays the relative particle fractions (of neutrons, protons, kaons, electrons, muons, and neutrinos) in trapped (lower panel) and untrapped (upper panel) matter as a function of the baryon density for several values of temperature, $T = 0$, 10, 30, and 50 MeV, obtained with $a_3 m_s = -222$ MeV and the micro-TBF. We note that temperature effects influence the populations mainly in the low-density region, and only slightly at high densities. Leptons are rather numerous at fairly low densities as a result of Fermi distributions at finite temperature.

The kaon condensate threshold density is only slightly dependent on the temperature, namely, 0.489, 0.490, 0.492, and 0.497 fm^{-3} at $T = 0$, 10, 30, and 50 MeV for untrapped matter and $T = 0.580$, 0.583, 0.589, and 0.629 fm^{-3} for trapped matter, respectively. The temperature influence on the kaon population is very small above the condensate threshold and concerns mainly the small fractions of thermal kaons present before the threshold. Above the critical density, thermal effects increase the population of protons and leptons in the untrapped case. We remark that, as usually found [5,15], in cold untrapped matter the presence of a kaon condensate pushes the proton fraction above the threshold for allowing fast URCA cooling.

There is a large difference between untrapped and trapped matter; in the latter, the kaon condensation sets in later and the kaon concentration remains lower. The major reason is the smaller nuclear asymmetry of trapped matter, which leads, according to Eq. (28), to a later kaon onset. [The direct dependence of the kaon effective mass on the nuclear asymmetry, Eq. (15), plays a minor role with the chosen interaction parameters.] In untrapped matter, the kaons immediately replace the leptons in compensating the charge of the protons; in trapped matter they cannot do that because the lepton number has to be kept fixed. Their effect is thus a moderate decrease in charged leptons, while the neutrino population increases. Overall, their importance is substantially reduced compared to the case of untrapped matter.

The dependence of the composition on the KN interaction strength is illustrated in Fig. 3, which shows the relative particle fractions in trapped (lower panels) and untrapped (upper panels) matter at $T = 30$ MeV for the three different values of the interaction parameter a_3 that we consider. The onset density of kaon condensation depends strongly on this parameter and ranges approximately from 0.4 to 0.6 fm^{-3} in untrapped matter and from 0.45 to 0.75 fm^{-3} in trapped matter. The fairly high onset densities for $a_3 m_s = -134$ MeV, corresponding to a small strangeness content of the proton, lie, however, in a region where the underlying concept of distinguishable baryons and mesons becomes doubtful, and also the simple chiral kaon-nucleon interaction would have to be extended.

Regarding the dependence of the particle concentrations on the TBF (micro or pheno) used, it was shown in the zero-temperature calculations in Ref. [17] that it is rather small, with only some slight differences at high density, where the micro-TBF is stiffer than the pheno-TBF. We therefore do not repeat this comparison here, but only report the final (P)NS structure results obtained with both TBFs in the next subsection.

B. (Proto)neutron star structure

Figure 4 shows the EOS $p(\rho)$ obtained with the micro-TBF (upper panels) and the pheno-TBF (lower panels) in the following cases: (a) no kaon condensate (left panels), (b) with kaon condensate, using $a_3 m_s = -134$ MeV (center panels), and (c) with kaon condensate, using $a_3 m_s = -222$ MeV (right panels). We consider three different strongly idealized stages of PNS evolution: (i) $T = 30$ MeV, $Y_e = 0.4$ [(black) dashed lines]—the initial hot and neutrino-trapped state; (ii) $T = 30$ MeV, $x_\nu = 0$ [(red) dotted lines]—the intermediate phase, lasting a few seconds, when most neutrinos have diffused out of the still hot environment; and (iii) $T = 0$ MeV, $x_\nu = 0$ [(green) solid lines]—the final state of a cold NS, formed after a few tens of seconds. This rather crude treatment of the different stages of PNS evolution can obviously be improved once more realistic temperature/trapping profiles become available. For the time being we consider it sufficient to reflect the gross qualitative features of the important evolution stages.

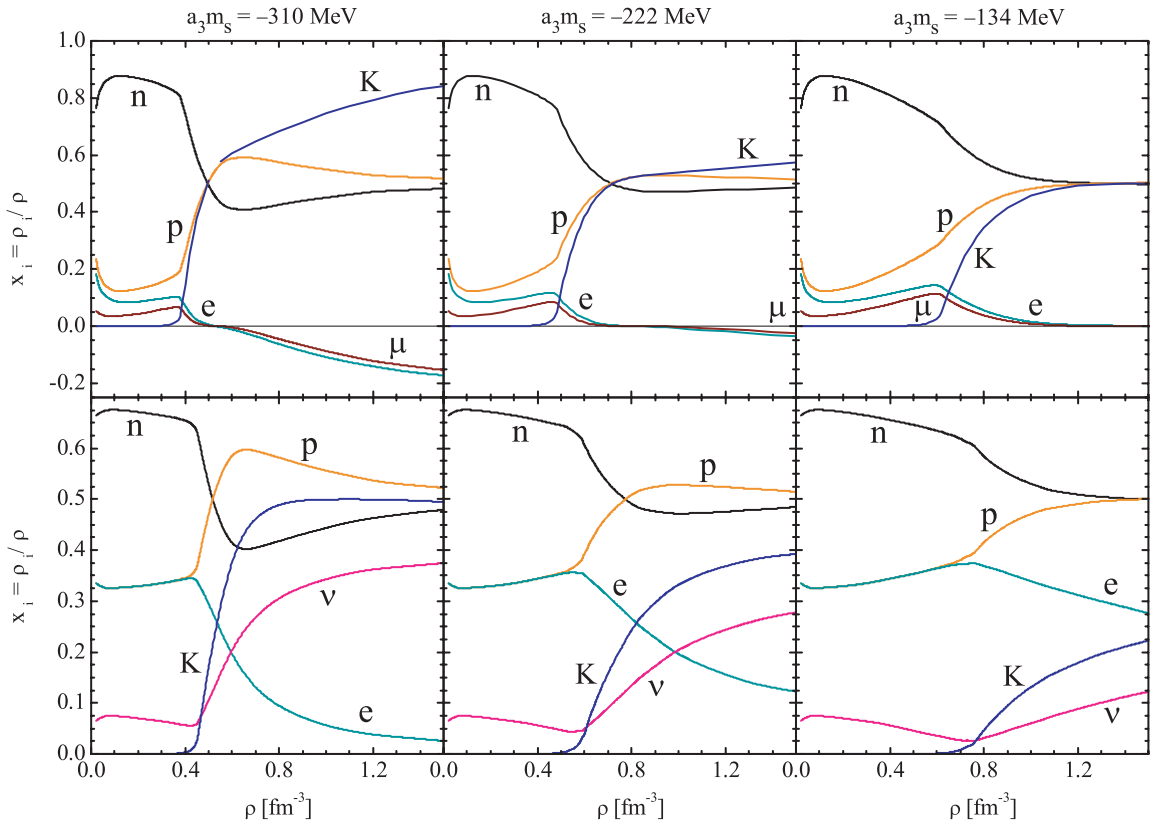

FIG. 3. (Color online) Particle fractions as a function of the baryon density in trapped ($Y_e = 0.4$; lower panels) and untrapped ($x_\nu = 0$; upper panels) β-stable matter, at temperature $T = 30$ MeV and with the micro-TBF for $a_3 m_s = -134$, -222, and -310 MeV. Negative values indicate an excess of antiparticles.

We observe that kaon condensation produces a general softening of the EOS with respect to the purely nucleonic case. The degree of softening increases with the value of the interaction parameter $|a_3 m_s|$. In the case with kaon condensate, neutrino trapping produces a stiffer EOS owing to the higher onset density of kaons and lower kaon abundance, as shown in

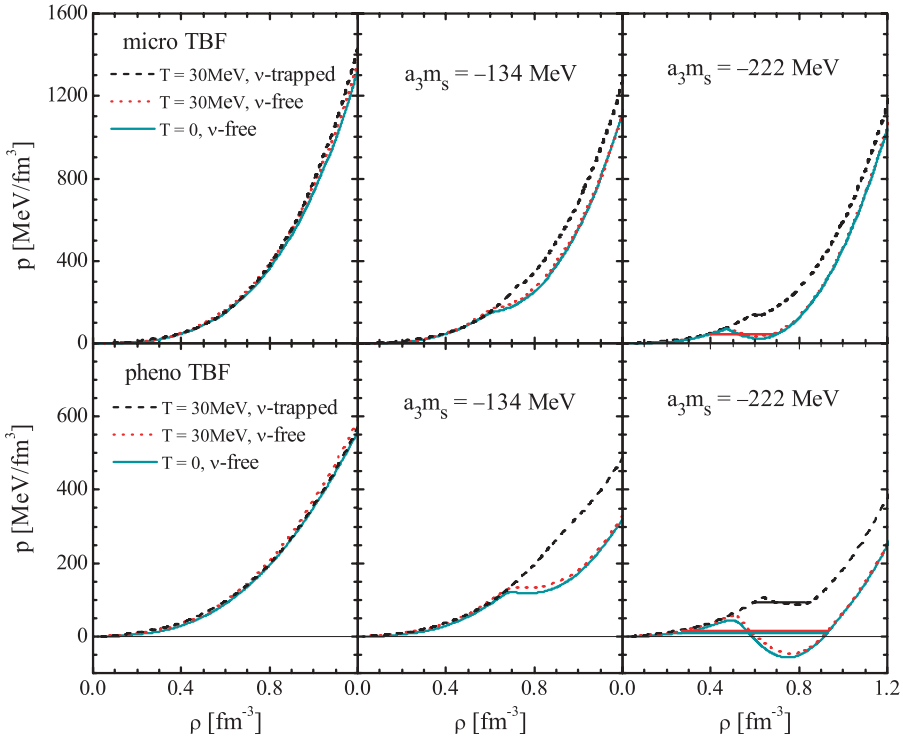

FIG. 4. (Color online) The pressure of β-stable matter under the conditions $T = 30$ MeV, $Y_e = 0.4$ [(black) dashed lines], $T = 30$ MeV, $x_\nu = 0$ [(red) dotted lines], and $T = 0$ MeV, $x_\nu = 0$ [(green) solid lines] is shown in the following cases: no kaon condensate (left panels), with kaon condensate and $a_3 m_s = -134$ MeV (center panels), or $a_3 m_s = -222$ MeV (right panels). Upper and lower panels display results obtained with the micro-TBF and the pheno-TBF, respectively. Solid line segments illustrate the Maxwell constructions.

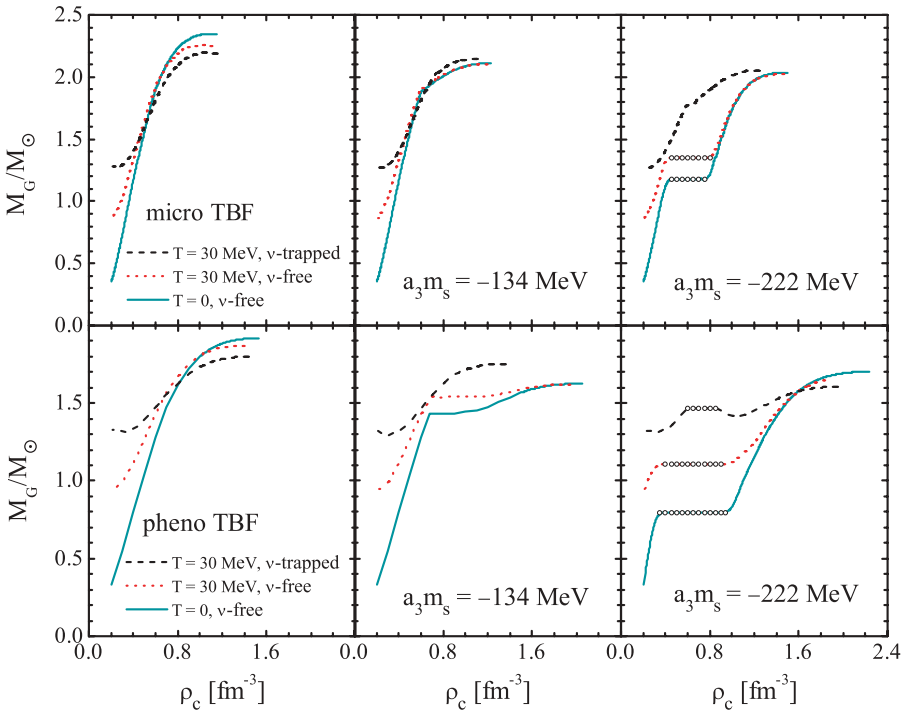

FIG. 5. (Color online) (Proto)neutron star gravitational mass - central density relations obtained with the micro-TBF (upper panels) and the pheno-TBF (lower panels) under the conditions $T = 30$ MeV, $Y_e = 0.4$ [(black) dashed lines], $T = 30$ MeV, $x_\nu = 0$ [(red) dotted lines], and $T = 0$ MeV, $x_\nu = 0$ [(green) solid lines] for $a_3 m_s = -222$ MeV, for $a_3 m_s = -134$ MeV, and without kaon condensation.

Fig. 3. This may lead a newly formed, hot PNS to metastability, that is, a delayed collapse while cooling down, as discussed in Refs. [8] and [11]. There is only a very small dependence of the EOS on the temperature, which thus plays a minor role in comparison with neutrino trapping. These considerations hold true also when pheno-TBFs are used in the baryonic EOS (Fig. 4; lower panels), where a softer increase in the pressure vs. density is observed compared to the case with micro-TBFs.

In some cases, the onset of the kaon-condensed phase produces a negative compressibility in the EOS. Following Migdal [47], we have performed a Maxwell construction to maintain a positive compressibility. This implies the formation of a region of constant pressure, comprised between two values of the baryon density, whose extension depends on the magnitude of $|a_3 m_s|$ [15]. It is indicated by horizontal lines in the relevant panels in Fig. 4.

These features are reflected in Fig. 5, where the corresponding gravitational mass - central density relations are plotted. The upper and lower panels show results obtained with the micro-TBF and the pheno-TBF, following the same notation as for Fig. 4. In the case without kaons (left panels), the maximum mass of the PNS is slightly smaller than that of the NS, because neutrino trapping reduces the asymmetry of β-stable matter. The presence of kaon condensation reverses the situation, and the PNS generally has a larger maximum mass than the NS, owing to the less softening effect of kaons in trapped matter. A delayed collapse scenario is therefore facilitated by the presence of a kaon condensate, as is indeed generally found [5,9,11]. Recall that a similar effect is also produced when hyperons are introduced in β-stable stellar matter [27].

Again, the effect of finite temperature is minor compared to that of trapping, so that a heavy PNS would be destabilized by loss of neutrinos early during its evolution. Regarding this feature, conclusions similar to ours can be drawn from the results of Refs. [8] and [9], whereas somewhat larger effects of finite temperature are claimed in Ref. [11]. However, in that case also a higher typical temperature was assumed in stage (ii) than in stage (i) of our evolution scenario, which accounts for at least some of the observed differences. It is clearly desirable to use a more realistic temperature profile for a more reliable evaluation of this feature in the future.

A rather extreme scenario is seen in the case of a quite soft nuclear EOS combined with a strong kaon condensate (lower-right panel in Fig. 5), where the maximum mass of the NS actually remains higher than that of the PNS and no delayed collapse could occur. A further consequence is the occurrence of gravitationally unstable sections in the mass-central density plot [see the (black) dashed curve], which was also observed in Refs. [5] and [9]. However, we consider this combination of extreme parameter choices unlikely, as it requires a very large density jump in the Maxwell construction (thus obliterating the soft part of the EOS) and also leads to unrealistically high central densities of the star. Furthermore, the case of a strong kaon condensate seems now to be excluded in the present model, as discussed before.

The global properties of the different configurations of (P)NSs are summarized in Table II. One notes that the theoretical predictions for the maximum masses depend most importantly on the nuclear EOS, whereas the effects of kaon condensation and/or neutrino trapping are of a smaller magnitude. Current observational values [48] suggest the existence of stars heavier than about 1.7 $M_\odot$, although their accurate confirmation is still eagerly awaited. Even if they are confirmed, somewhat higher values, about 2 $M_\odot$ would be required to really discriminate between different nuclear EOS.

TABLE II. Properties of (proto)neutron stars.

	$a_3 m_s$ (MeV)	Micro-TBF		Pheno-TBF	
		$M_{\max}/M_\odot$	ρ_c/ρ_0	$M_{\max}/M_\odot$	ρ_c/ρ_0
Trapped	–	2.19	6.29	1.80	8.24
$T = 30$ MeV	−134	2.14	6.24	1.75	7.82
	−222	2.05	7.12	1.61	11.47
Untrapped	–	2.26	6.00	1.87	7.94
$T = 30$ MeV	−134	2.10	6.76	1.62	11.17
	−222	2.02	8.35	1.67	12.53
Untrapped	–	2.34	6.29	1.92	8.76
$T = 0$	−134	2.11	6.88	1.62	11.76
	−222	2.03	8.47	1.70	12.94

V. SUMMARY

In conclusion, we have presented microscopic calculations and convenient parametrizations of the EOS of hot asymmetric nuclear matter within the framework of the BHF approach with two different nuclear TBFs. We then investigated the EOS as well as the consequences of including kaon condensation in hot and neutrino-trapped NS matter, employing a standard chiral model at finite temperature. Effects of finite temperature are thus included consistently in both the nucleonic and the kaonic part of the interaction.

Our results are qualitatively in agreement with those obtained with more phenomenological approaches [8,9], although the quantitative predictions turn out to be different. In particular, we found that, also in our microscopic approach, finite temperature plays a minor role compared to neutrino trapping, which generally decreases the stellar maximum mass in the absence of a kaon condensate and increases it when a condensate is present. This is because of the reduced appearance of kaons in trapped vs. untrapped matter. Global PNS properties are, however, determined primarily by the *nucleonic* part of the EOS.

Furthermore, if recent very small values for the strangeness content of the proton are confirmed, kaon condensation in the present model sets in only at a critical density $\rho_c^K \gtrsim 4\rho_0$, whereas in the same BHF framework hyperons appear at $\rho_c^Y \approx (2\text{–}3)\rho_0$ [36,39,49] and would then completely suppress the kaon degree of freedom. In any case, the maximum mass of a (P)NS is greatly reduced by the appearance of strangeness in the relevant dense environment, in the form of either kaons or hyperons; and in both cases a delayed collapse scenario appears very probable.

ACKNOWLEDGMENTS

This work is supported in part by the National Natural Science Foundation of China (Grant Nos. 10605018, 10905048, and 10975116), the Knowledge Innovation Project (Grant No. KJCX3-SYW-N2) of the Chinese Academy of Sciences, the Program for New Century Excellent Talents in University (Grant No. NCET-07-0730), the Asia-Europe Link project [Grant No. CN/ASIA-LINK/008(94791)] of the European Commission, and COMPSTAR, a research networking program of the European Science Foundation.

[1] D. B. Kaplan and A. E. Nelson, Phys. Lett. **B175**, 57 (1986); Nucl. Phys. **A479**, 273 (1988).
[2] H. D. Politzer and M. B. Wise, Phys. Lett. **B273**, 156 (1991).
[3] G. E. Brown, K. Kubodera, M. Rho, and V. Thorsson, Phys. Lett. **B291**, 355 (1992).
[4] C. H. Lee, G. E. Brown, D. P. Min, and M. Rho, Nucl. Phys. **A585**, 401 (1995); C. H. Lee, Phys. Rep. **275**, 255 (1996), and references therein; G. E. Brown, C. H. Lee, and M. Rho, *ibid.* **462**, 1 (2008).
[5] V. Thorsson, M. Prakash, and J. M. Lattimer, Nucl. Phys. **A572**, 693 (1994); **A574**, 851 (1994).
[6] P. J. Ellis, R. Knorren, and M. Prakash, Phys. Lett. **B349**, 11 (1995).
[7] N. K. Glendenning and J. Schaffner-Bielich, Phys. Rev. Lett. **81**, 4564 (1998); Phys. Rev. C **60**, 025803 (1999).
[8] M. Prakash, I. Bombaci, M. Prakash, P. J. Ellis, J. M. Lattimer, and R. Knorren, Phys. Rep. **280**, 1 (1997).
[9] T. Tatsumi and M. Yasuhira, Phys. Lett. **B441**, 9 (1998); Nucl. Phys. **A653**, 133 (1999); M. Yasuhira and T. Tatsumi, *ibid.* **A690**, 769 (2001); T. Muto, M. Yasuhira, T. Tatsumi, and N. Iwamoto, Phys. Rev. D **67**, 103002 (2003).
[10] T. Muto, T. Tatsumi, and N. Iwamoto, Phys. Rev. D **61**, 063001, 083002 (2000).
[11] J. A. Pons, S. Reddy, P. J. Ellis, M. Prakash, and J. M. Lattimer, Phys. Rev. C **62**, 035803 (2000); J. A. Pons, J. A. Miralles, M. Prakash, and J. M. Lattimer, Astrophys. J. **553**, 382 (2001).
[12] A. Ramos, J. S. Bielich, and J. Wambach, Lect. Notes Phys. **578**, 175 (2001).
[13] J. Carlson, H. Heiselberg, and V. R. Pandharipande, Phys. Rev. C **63**, 017603 (2000).
[14] T. Norsen and S. Reddy, Phys. Rev. C **63**, 065804 (2001).
[15] S. Kubis and M. Kutschera, Nucl. Phys. **A720**, 189 (2003).
[16] W. Zuo, A. Li, Z. H. Li, and U. Lombardo, Phys. Rev. C **70**, 055802 (2004).
[17] A. Li, G. F. Burgio, U. Lombardo, and W. Zuo, Phys. Rev. C **74**, 055801 (2006).
[18] M. Fukugita, Y. Kuramashi, M. Okawa, and A. Ukawa, Phys. Rev. D **51**, 5319 (1995).
[19] S. J. Dong, J.-F. Lagaë, and K. F. Liu, Phys. Rev. D **54**, 5496 (1996).
[20] S. Güsken *et al.*, Phys. Rev. D **59**, 054504 (1999).
[21] V. E. Lyubovitskij, T. Gutsche, A. Faessler, and E. G. Drukarev, Phys. Rev. D **63**, 054026 (2001).
[22] H. Ohki *et al.*, Phys. Rev. D **78**, 054502 (2008).
[23] R. Knorren, M. Prakash, and P. J. Ellis, Phys. Rev. C **52**, 3470 (1995); J. Schaffner and I. N. Mishustin, *ibid.* **53**, 1416 (1996); T. Muto, *ibid.* **77**, 015810 (2008).
[24] T. W. Baumgarte, S. L. Shapiro, and S. A. Teukolsky, Astrophys. J. **458**, 680 (1996).
[25] T. Takatsuka, Prog. Theor. Phys. **95**, 901 (1996).
[26] K. Strobel, C. Schaab, and M. K. Weigel, Astron. Astrophys. **350**, 497 (1999); K. Strobel and M. K. Weigel, *ibid.* **367**, 582 (2001).
[27] O. E. Nicotra, M. Baldo, G. F. Burgio, and H.-J. Schulze, Astron. Astrophys. **451**, 213 (2006); Phys. Rev. D **74**, 123001 (2006).

[28] G. F. Burgio and H.-J. Schulze, Phys. At. Nucl. **72**, 1197 (2009).
[29] A. Lejeune, P. Grangé, M. Martzolff, and J. Cugnon, Nucl. Phys. **A453**, 189 (1986).
[30] I. Bombaci and U. Lombardo, Phys. Rev. C **44**, 1892 (1991); W. Zuo, I. Bombaci, and U. Lombardo, *ibid.* **60**, 024605 (1999).
[31] M. Baldo, *Nuclear Methods and the Nuclear Equation of State*. International Review of Nuclear Physics, Vol. 8 (World Scientific, Singapore, 1999).
[32] M. Baldo and L. S. Ferreira, Phys. Rev. C **59**, 682 (1999).
[33] R. B. Wiringa, V. G. J. Stoks, and R. Schiavilla, Phys. Rev. C **51**, 38 (1995).
[34] P. Grangé, A. Lejeune, M. Martzolff, and J.-F. Mathiot, Phys. Rev. C **40**, 1040 (1989).
[35] W. Zuo, A. Lejeune, U. Lombardo, and J.-F. Mathiot, Nucl. Phys. **A706**, 418 (2002); Z. H. Li, U. Lombardo, H.-J. Schulze, and W. Zuo, Phys. Rev. C **77**, 034316 (2008).
[36] Z. H. Li and H.-J. Schulze, Phys. Rev. C **78**, 028801 (2008).
[37] J. Carlson, V. R. Pandharipande, and R. B. Wiringa, Nucl. Phys. **A401**, 59 (1983); R. Schiavilla, V. R. Pandharipande, and R. B. Wiringa, *ibid.* **A449**, 219 (1986).
[38] M. Baldo, I. Bombaci, and G. F. Burgio, Astron. Astrophys. **328**, 274 (1997); X. R. Zhou, G. F. Burgio, U. Lombardo, H.-J. Schulze, and W. Zuo, Phys. Rev. C **69**, 018801 (2004).
[39] M. Baldo, G. F. Burgio, and H.-J. Schulze, Phys. Rev. C **58**, 3688 (1998).
[40] S. L. Shapiro and S. A. Teukolsky, *Black Holes, White Dwarfs, and Neutron Stars* (John Wiley and Sons, New York, 1983).
[41] A. Burrows and J. M. Lattimer, Astrophys. J. **307**, 178 (1986).
[42] J. A. Pons, S. Reddy, M. Prakash, J. M. Lattimer, and J. A. Miralles, Astrophys. J. **513**, 780 (1999); L. Villain, J. A. Pons, P. Cerdá-Durán, and E. Gourgoulhon, Astron. Astrophys. **418**, 283 (2004).
[43] J. W. Negele and D. Vautherin, Nucl. Phys. **A207**, 298 (1973).
[44] G. Baym, C. Pethick, and D. Sutherland, Astrophys. J. **170**, 299 (1971).
[45] R. Feynman, F. Metropolis, and E. Teller, Phys. Rev. **75**, 1561 (1949).
[46] D. Gondek, P. Haensel, and J. L. Zdunik, Astron. Astrophys. **325**, 217 (1997).
[47] A. B. Migdal, in *Mesons in Nuclei*, Vol. 3, edited by M. Rho and D. Wilkinson (North-Holland, Amsterdam, 1979).
[48] J. M. Lattimer and M. Prakash, Phys. Rep. **442**, 109 (2007).
[49] M. Baldo, G. F. Burgio, and H.-J. Schulze, Phys. Rev. C **61**, 055801 (2000); H.-J. Schulze, A. Polls, A. Ramos, and I. Vidaña, *ibid.* **73**, 058801 (2006).